

Thermodynamic properties of $\text{Bi}_2\text{Sr}_2\text{CaCu}_2\text{O}_{8+\delta}$ calculated from the electronic dispersion

J. G. Storey,¹ J. L. Tallon,^{1,2} and G. V. M. Williams²

¹*School of Chemical and Physical Sciences, Victoria University, P.O. Box 600, Wellington 6140, New Zealand*

²*MacDiarmid Institute, Industrial Research Ltd., P.O. Box 31310, Lower Hutt 5040, New Zealand*

(Received 13 December 2007; published 19 February 2008)

The electronic dispersion for $\text{Bi}_2\text{Sr}_2\text{CaCu}_2\text{O}_{8+\delta}$ has been determined from angle-resolved photoemission spectroscopy (ARPES). From this dispersion, we calculate the entropy and superfluid density. Even with no adjustable parameters, we obtain an exceptional match with experimental data across the entire phase diagram, thus indirectly confirming both the ARPES and thermodynamic data. The van Hove singularity is crossed in the overdoped region, giving a distinctive linear-in- T temperature dependence in the superfluid density there.

DOI: [10.1103/PhysRevB.77.052504](https://doi.org/10.1103/PhysRevB.77.052504)

PACS number(s): 74.25.Bt, 74.25.Jb, 74.62.Dh, 74.72.-h

The generic doping dependence of the thermodynamic, electrodynamic, and transport properties of high- T_c superconductors remains a puzzle despite many years of study. Their unusual behavior is often taken to be a signature of exotic physics, yet it should be related to the electronic energy-momentum dispersion obtained, for example, from angle-resolved photoemission spectroscopy (ARPES). These studies indicate the presence of an extended van Hove saddle-point singularity¹ situated at the $(0, \pi)$ point together with a normal-state pseudogap² as common features in the electronic band structure. The pseudogap (PG) exhibits a reduction in the density of states (DOS) at the Fermi level which is believed to develop into a fully nodal gap at low temperature.³

In theories based on the so-called van Hove scenario,⁴ the superconducting (SC) transition temperature T_c is enhanced by the proximity of a van Hove singularity (vHs). These theories assume that the vHs sweeps through the Fermi level E_F at optimal doping ($p=0.16$), indeed causing the peak in $T_c(p)$. However, ARPES studies on Bi-2201 (Ref. 5) show that the vHs crosses E_F in the deeply overdoped side of the phase diagram. For a bilayer cuprate like Bi-2212, the weak coupling between the layers splits the bands near $(\pi, 0)$ into an upper antibonding band and a lower bonding band. ARPES studies on Bi-2212 (Ref. 6) suggest that the antibonding vHs crosses at around $p=0.225$ where $T_c \approx 60$ K, i.e., near the limit for overdoping in this material. The vHs crossing should profoundly affect all physical properties. However, doubts remain. Most of the ARPES intensity comes from the outermost CuO_2 layer: surface states could seriously modulate the results, and cleavage could lower the surface doping state.

Here, we have used thermodynamics (a bulk property) as a window on the electronic structure to independently check the main ARPES results (a surface property), and because the specific heat work of Loram *et al.*⁷ has never been independently confirmed (indeed, it has been contradicted by Tutsch *et al.*⁸), our present study effectively provides a check on that also. We have calculated the p and T dependences of the entropy and superfluid density of Bi-2212 using an ARPES-derived energy dispersion. Inputs are taken directly, and only, from ARPES in order to determine the implications of these data. Our calculations confirm the ARPES results, giving a consistent picture of the thermodynamic properties in terms of a proximate vHs.

We assume Fermi-liquid-like, mean-field, weak-coupling physics in spite of expectations to the contrary. In defense, (i) the thermodynamics at low T is dominated by the nodal regions of the Fermi surface where quasiparticles are long lived, and (ii) the Wilson ratio relating spin susceptibility to S/T (where S is the electronic entropy) is almost exactly that for nearly free electrons across a wide range of p and T .⁷ Moreover, non-mean-field BCS-like behavior is generally inferred from the unusual $2\Delta/k_B T_c$ ratio which grows with underdoping. However, it has always been our view,⁹ and is now confirmed,^{10,11} that the large and growing energy gap used here is the $(\pi, 0)$ PG, not the SC gap. Once the PG is properly included in the problem, then $2\Delta/k_B T_c$ is well behaved. We do not treat fluctuations which are confined to $T_c \pm 15$ K (Ref. 12) and are a minor embellishment.

For Bi-2212, we employ a two-dimensional bilayer dispersion $\epsilon_{\mathbf{k}}$ provided by the authors of Ref. 6, which was obtained from tight binding fits to high-resolution ARPES data. The DOS per spin at energy E is given by

$$N(E) = N_k^{-1} \sum_{\mathbf{k}} \delta(\epsilon_{\mathbf{k}} - E). \quad (1)$$

The molar entropy for weakly interacting fermions is¹³

$$S = -2R \int [f \ln f + (1-f) \ln(1-f)] N(E) dE, \quad (2)$$

where f is the Fermi-Dirac distribution function and R is the gas constant. The chemical potential $\mu(T)$ is calculated self-consistently such that the carrier concentration n is T independent. n is given by

$$n = (2/V_A) \int f(E) N(E) dE, \quad (3)$$

where V_A is the atomic volume per formula unit.

The inset of Fig. 1 shows the Fermi surface in the first Brillouin zone. The PG first forms near $(\pi, 0)$, leaving ungapped Fermi arcs¹⁴ between. With decreasing T , the Fermi arcs narrow and the gap seems to become nodal at $T=0$. We, thus, adopt a PG of the form

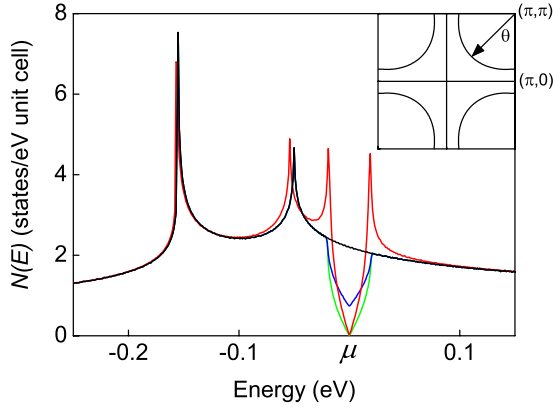


FIG. 1. (Color online) The DOS calculated from the Bi-2212 bilayer dispersion determined by ARPES measurements (black). Also shown is a 20 meV pseudogap at 0 K (green) and 100 K (blue), and a 20 meV SC gap at 0 K (red). Inset: The Fermi surface in the (k_x, k_y) plane showing the angle θ .

$$E_g = \begin{cases} E_{g,max} \cos\left(\frac{2\pi\theta}{4\theta_0}\right) & (\theta < \theta_0) \\ E_{g,max} \cos\left(\frac{2\pi(\theta - \pi/2)}{4\theta_0}\right) & \left(\theta > \frac{\pi}{2} - \theta_0\right) \\ 0 & \text{otherwise,} \end{cases} \quad (4)$$

where

$$\theta_0 = \frac{\pi}{4} \left[1 - \tanh\left(\frac{T}{T^*}\right) \right] \quad (5)$$

and $T^* = E_{g,max}/k_B$. θ is the angle shown in Fig. 1.

Equation (5) models the observed temperature dependence of the Fermi arc length.³ At $T=0$, $\theta_0 = \pi/4$ and the PG is fully nodal. As T rises, θ_0 decreases, resulting in a “filling-in” of the PG and the growth of the Fermi arcs. This model is based on results by Kanigel *et al.*³ that show the Fermi arcs collapsing linearly as a function of T/T^* , extrapolating to zero as $T \rightarrow 0$. However, we note an important feature of our model. The Kanigel data show the PG opening abruptly at $T=T^*$. A PG which fills completely at T^* would result in a jump in the specific heat coefficient γ at T^* , which is not observed. The smooth evolution of the tanh function in Eq. (5) overcomes this problem. The PG is states-non-conserving, i.e., unlike the SC gap, there is no pileup of states outside the gap (see Fig. 1). This is implemented by eliminating states with energies $E < E_g$ from the summations.

Figure 1 shows the DOS calculated from the bilayer dispersion. The bonding vHs lies 105 meV below the antibonding vHs. Also shown is a 20 meV PG at $T=0$ and 100 K illustrating the gap filling with T . The gap node is pinned to the chemical potential at all T .

The entropy in the SC state has been modeled using a d -wave gap of the form $\Delta_{\mathbf{k}} = \frac{1}{2}\Delta_0 g_{\mathbf{k}}$, where $g_{\mathbf{k}} = \cos k_x - \cos k_y$. The dispersion in the presence of the SC gap is given by $E_{\mathbf{k}} = \sqrt{\epsilon_{\mathbf{k}}^2 + \Delta_{\mathbf{k}}^2}$, and $\Delta_0(T)$ is determined from the self-consistent weak-coupling BCS gap equation¹³

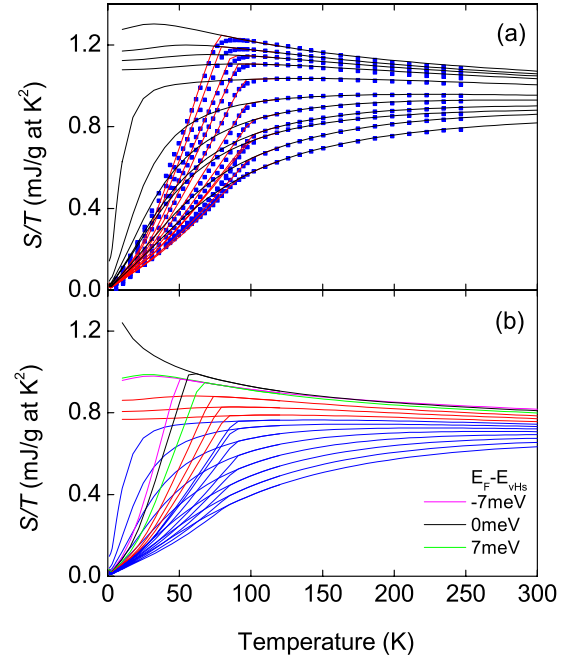


FIG. 2. (Color online) (a) Refined normal-state (black) and SC-state (red) fits to the electronic entropy data (Ref. 7) for Bi-2212. For clarity, every 20th data point only is shown. Each curve represents a different doping level from $p=0.129$ to 0.209 . (b) Unrefined absolute entropy curves with no fitting parameter.

$$1 = \frac{V}{2} \sum_{\mathbf{k}} \frac{|g_{\mathbf{k}}|^2}{E_{\mathbf{k}}} \tanh\left(\frac{E_{\mathbf{k}}}{2k_B T}\right). \quad (6)$$

We adopt a pairing potential of the form $V_{\mathbf{k}\mathbf{k}'} = V g_{\mathbf{k}} g_{\mathbf{k}'}$. The amplitude V is assumed to be constant ($=125$ meV) up to an energy cutoff ω_c chosen such that T_c matches the experimentally observed value. The PG is not included in the process of calculating $\Delta_0(T)$.

The superfluid density ρ_s is proportional to the inverse square of the penetration depth given by¹⁵

$$\frac{1}{\lambda_{ab}^2} = \frac{\mu_0 e^2 n}{4\pi\hbar^2} \sum_{\mathbf{k}} \left[\left(\frac{\partial \epsilon_{\mathbf{k}}}{\partial k_x} \right)^2 \frac{\Delta_{\mathbf{k}}^2}{E_{\mathbf{k}}^2} - \frac{\partial \epsilon_{\mathbf{k}}}{\partial k_x} \frac{\partial \Delta_{\mathbf{k}}}{\partial k_x} \frac{\Delta_{\mathbf{k}} \epsilon_{\mathbf{k}}}{E_{\mathbf{k}}^2} \right] \times \left[\frac{1}{E_{\mathbf{k}}} - \frac{\partial}{\partial E_{\mathbf{k}}} \right] \tanh\left(\frac{E_{\mathbf{k}}}{2k_B T}\right). \quad (7)$$

The summation in Eqs. (6) and (7) is performed over both the bonding and antibonding bands and Δ is assumed to be the same for both bands.¹⁶

The data points in Fig. 2(a) show the normal- and SC-state entropy data of Loram *et al.*⁷ Figure 2(b) shows the absolute entropy calculated from the dispersion with no fitting parameters. We merely specified the location of E_F relative to E_{vHs} at two points only: in the overdoped region from Kaminski *et al.*⁶ and in the underdoped region from Kordyuk *et al.*,¹⁷ and interpolated between. The doping dependence of E_g is obtained from the reported leading-edge ARPES gap at 100 K.⁹ The overall T and p dependences of the experimental data are reproduced superbly, with absolute values just a fac-

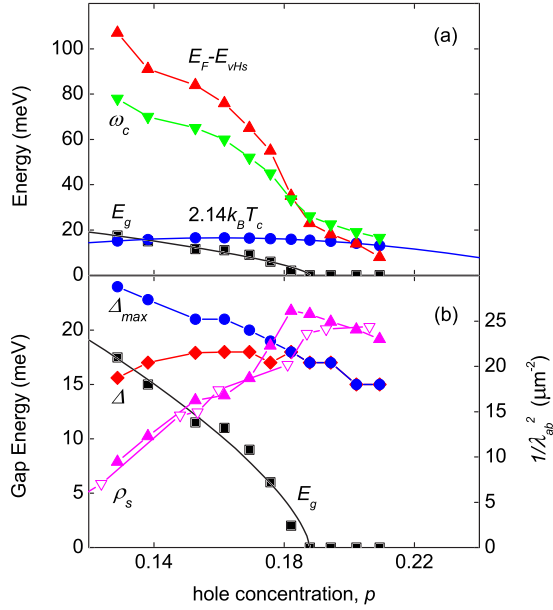


FIG. 3. (Color online) (a) $E_F - E_{vHs}$ (up triangles) (the vHs will cross E_F at $p \approx 0.22$), pairing potential energy cutoff ω_c (down triangles), pseudogap magnitude E_g (squares) and a fit given by Eq. (8), and the measured T_c multiplied by $2.14k_B$ (circles). (b) Maximum gap as measured from the DOS at 10 K (circles), SC gap measured from the DOS at 10 K in the absence of a pseudogap (diamonds), calculated superfluid density at 10 K (up triangles), and measured low- T Bi-2212 superfluid density (Ref. 22) (down triangles).

tor of 3/4 lower. This is our first main result. S/T rises with doping and reaches its maximum at the vHs as observed also in $\text{La}_{2-x}\text{Sr}_x\text{CuO}_4$.⁷ Figure 2(b) is, by the way, inconsistent with the data of Tutsch *et al.*,⁸ which failed to show a PG.

In Fig. 2(a), we have rescaled the computed entropy by the constant factor of 4/3 and refined the fit using E_F and $E_{g,max}$ as fitting parameters. These refinements do not alter the overall behavior and are tightly constrained. For example, the normal-state fits to the four most overdoped data sets were obtained by adjusting a single parameter, namely, E_F , as are the high- T asymptotes for all data sets. At the most overdoped, E_F is only 8 meV above the antibonding band vHs.

As the doping decreases, the vHs recedes from E_F , resulting in a decrease in the number of states within $k_B T$ of μ and a corresponding reduction in entropy. However, as the doping is further reduced, the recession of the vHs from E_F is no longer able to account for the observed decrease in entropy alone and the second adjustable parameter, the PG magnitude E_g , is introduced. This results in the progressive downturn in the normal-state S/T as temperature decreases. The deduced values of $E_F - E_{vHs}$ and E_g are plotted versus doping in Fig. 3(a) along with the measured T_c . The doping level has been determined from the empirical relation¹⁸ $p = 0.16 \pm 0.11 \sqrt{1 - T_c/T_{c,max}}$. The fits suggest that the antibonding vHs will cross E_F near $p = 0.22$, in full agreement with recent ARPES studies⁶ on Bi-2212 where the crossing occurs at $p = 0.225$. This is our next key result.

The PG is observed to open at critical doping

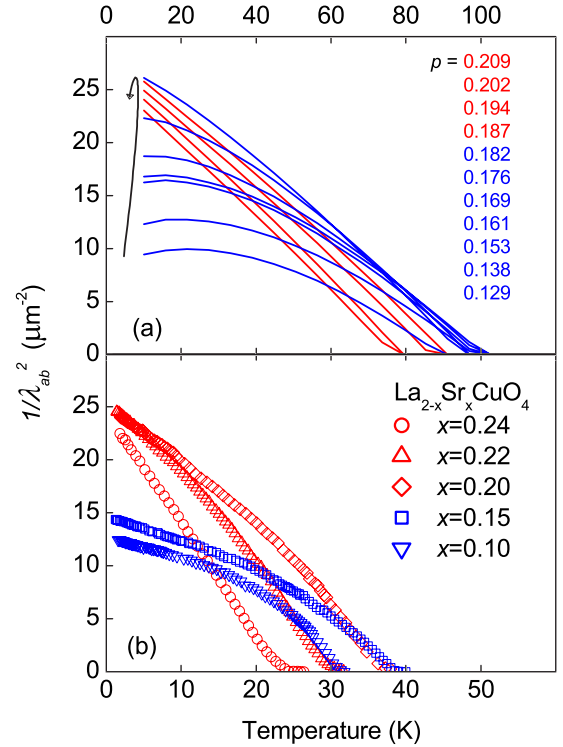


FIG. 4. (Color online) Superfluid density (a) computed using parameters from the entropy fits in Fig. 2. The arrow indicates increasing doping. (b) Experimental data for La-214 (Ref. 28). Curves or data in which the PG is present are shown in blue.

$p_{crit} = 0.188$, in agreement with previous analyses.^{7,19} E_g has been fitted with the following equation:

$$T^*(p) = E_g/k_B = T_0^*(1 - p/p_{crit})^{1-\alpha} \quad (8)$$

with $T_0^* = 443.7$ K and $\alpha = 0.317$. These values agree with the results of Naqib *et al.*,²⁰ who determined $T^*(p)$ of YBCO from transport studies. A fit to their data gives $T_0^* = 510$ K and $\alpha = 0.2$. The sublinear behavior of $T^*(p)$ is expected if p_{crit} is a quantum critical point.²¹

From the SC-state fits, the energy cutoff ω_c falls linearly with $E_F - E_{vHs}$. In particular, ω_c (meV) = $10.96 + 0.637(E_F - E_{vHs})$, with correlation coefficient $R = 0.99945$. This rapid fall in ω_c suggests a magnetic or magnetically enhanced pairing rather than phononic.

Figure 3(b) shows the magnitude of the combined SC gap and PG, Δ_{max} , measured from the calculated DOS at 10 K. Δ_{max} increases with decreasing doping just as observed from ARPES,²³ tunnelling,²⁴ and Raman scattering.²⁵ Also plotted is the SC gap magnitude Δ , determined by setting $E_g = 0$ and measuring the gap in the calculated DOS at 10 K. The magnitude is smaller than typically observed because of the weak-coupling assumption for which $2\Delta/k_B T_c = 4.28$. The gap Δ rises and falls in conjunction with the observed T_c . Note that the experimentally observed monotonic increase in the gap magnitude with decreasing doping is, here, seen to be associated with the PG, and not the SC gap as generally believed. The behavior here is consistent with the two-gap picture presented by Deutscher²⁶ and, more recently, by Le

Tacon *et al.*,¹¹ but has been a feature of our work for a long time.^{9,19,27}

By using the parameters obtained from the entropy fits, the superfluid density has been calculated using Eq. (7) with no further adjustable parameters, and is shown in Fig. 4(a). For comparison (in the absence of data for Bi-2212), Fig. 4(b) shows $\rho_s(T)$ for $\text{La}_{2-x}\text{Sr}_x\text{CuO}_4$ (La-214) determined by ac-susceptibility studies²⁸ on grain-aligned samples. The agreement is excellent. The increasing linearity of $\rho_s(T)$ with overdoping can now be understood in terms of the approach to the vHs, where full linearity occurs. (The crossing of the vHs in La-214 can also be inferred from the maximum in the entropy at $p=0.24$.⁷) The opening of the PG leads to the decline in ρ_s observed below $p=0.19$. This is clearly illustrated by the plot of $\rho_s(10\text{ K})$ vs p in Fig. 3(b). The overall doping dependence and absolute magnitude of $\rho_s(10\text{ K})$ concurs almost exactly with experimental data for Bi-2212,²² also shown. This is our third key result. We recall that no fitting parameters are used in Eq. (7). It is remarkable that S/T and $\rho_s(T)$ are so similar in La-214, Bi-2212, and, indeed, $\text{Y}_{1-x}\text{Ca}_x\text{Ba}_2\text{Cu}_3\text{O}_{7-\delta}$ despite the significant differences in bare band structure. The renormalized dispersion near E_F seems to lead to a universal phenomenology which calls for theoretical explanation.

In the underdoped data, the downturn seen at low T and p in the calculated $\rho_s(T)$ curves arises from the closing of the

Fermi arcs and is not observed in the experimental data, which show an upturn at low T and p . To us this indicates that the Fermi arc picture is, at best, incomplete. We will discuss this elsewhere.

In summary, we have calculated the entropy and superfluid density of Bi-2212 directly from an ARPES-derived dispersion. The T and p dependences of both can be fully explained by the combined effects of a proximate vHs and the opening of a normal-state pseudogap. These results provide indirect confirmation of both the (bulk) thermodynamic and (surface) ARPES data. Entropy fits indicate that the antibonding vHs crosses E_F near $p=0.22$, in agreement with recent ARPES results. The superfluid density calculated using no adjustable parameters shows excellent agreement with experimental data and exhibits a distinctive overall linear-in- T behavior at the vHs. The universal renormalized phenomenology in the various cuprates, despite their differences in bare band structure, is a key conclusion that demands theoretical explanation. It also remains a theoretical challenge to understand why the Fermi-liquid approach is so successful in a strongly correlated system.

Thanks are due to A. Kaminski for the dispersion parameters and also to N. W. Ashcroft for much discussion and many helpful comments on this work.

-
- ¹J. Ma, C. Quitmann, R. J. Kelley, P. Almeras, H. Berger, G. Margaritondo, and M. Onellion, *Phys. Rev. B* **51**, 3832 (1995).
²H. Ding, T. Yokoya, J. C. Campuzano, T. Takahashi, M. Randeria, M. R. Norman, T. Mochiku, K. Kadowaki, and J. Giapintzakis, *Nature (London)* **382**, 51 (1996).
³A. Kanigel *et al.*, *Nat. Phys.* **2**, 447 (2006).
⁴R. S. Markiewicz, *J. Phys. Chem. Solids* **58**, 1179 (1997).
⁵T. Kondo, T. Takeuchi, T. Yokoya, S. Tsuda, S. Shin, and U. Mizutani, *J. Electron Spectrosc. Relat. Phenom.* **137-140**, 663 (2004).
⁶A. Kaminski, S. Rosenkranz, H. M. Fretwell, M. R. Norman, M. Randeria, J. C. Campuzano, J. M. Park, Z. Z. Li, and H. Raffy, *Phys. Rev. B* **73**, 174511 (2006).
⁷J. W. Loram, J. Luo, J. R. Cooper, W. Y. Liang, and J. L. Tallon, *J. Phys. Chem. Solids* **62**, 59 (2001).
⁸U. Tutsch, P. Schweiss, H. Wühl, B. Obst, and T. Wolf, *Eur. Phys. J. B* **41**, 471 (2004).
⁹J. L. Tallon and J. W. Loram, *Physica C* **349**, 53 (2001).
¹⁰K. Tanaka *et al.*, *Science* **314**, 1910 (2006).
¹¹M. Le Tacon, A. Sacuto, A. Georges, G. Kotliar, Y. Gallais, D. Colson, and A. Forget, *Nat. Phys.* **2**, 537 (2006).
¹²J. W. Loram, J. L. Tallon, and W. Y. Liang, *Phys. Rev. B* **69**, 060502(R) (2004).
¹³R. D. Parks, *Superconductivity* (Dekker, New York, 1969), Vol. 1.
¹⁴M. R. Norman *et al.*, *Nature (London)* **392**, 157 (1998).
¹⁵D. E. Sheehy, T. P. Davis, and M. Franz, *Phys. Rev. B* **70**, 054510 (2004).
¹⁶S. V. Borisenko, A. A. Kordyuk, T. K. Kim, S. Legner, K. A. Nenkov, M. Knupfer, M. S. Golden, J. Fink, H. Berger, and R. Follath, *Phys. Rev. B* **66**, 140509(R) (2002).
¹⁷A. A. Kordyuk, S. V. Borisenko, M. Knupfer, and J. Fink, *Phys. Rev. B* **67**, 064504 (2003).
¹⁸M. R. Presland, J. L. Tallon, R. G. Buckley, R. S. Liu, and N. E. Flower, *Physica C* **176**, 95 (1991).
¹⁹J. L. Tallon, G. V. M. Williams, M. P. Staines, and C. Bernhard, *Physica C* **235-240**, 1821 (1994).
²⁰S. H. Naqib, J. R. Cooper, J. L. Tallon, R. S. Islam, and R. A. Chakalov, *Phys. Rev. B* **71**, 054502 (2005).
²¹J. Zaanen and B. Hosseinkhani, *Phys. Rev. B* **70**, 060509(R) (2004).
²²W. Anukool, Ph. D. thesis, University of Cambridge, England, 2003.
²³J. C. Campuzano *et al.*, *Phys. Rev. Lett.* **83**, 3709 (1999).
²⁴N. Miyakawa, P. Guptasarma, J. F. Zasadzinski, D. G. Hinks, and K. E. Gray, *Phys. Rev. Lett.* **80**, 157 (1998).
²⁵C. Kendziora and A. Rosenberg, *Phys. Rev. B* **52**, R9867 (1995).
²⁶G. Deutscher, *Nature (London)* **397**, 410 (1999).
²⁷J. Loram, K. A. Mirza, J. R. Cooper, W. Y. Liang, and J. M. Wade, *J. Supercond.* **7**, 243 (1994).
²⁸C. Panagopoulos, B. D. Rainford, J. R. Cooper, W. Lo, J. L. Tallon, J. W. Loram, J. Betouras, Y. S. Wang, and C. W. Chu, *Phys. Rev. B* **60**, 14617 (1999).